The carbon sink potential of southern China after two decades of afforestation

Xuemei Zhang[1,2,3], Martin Brandt[4], Yuemin Yue[1,2,*], Xiaowei Tong[1,4], Kelin Wang[1,2,*], Rasmus Fensholt[4]

[1] Key Laboratory for Agro-ecological Processes in Subtropical Region, Institute of Subtropical Agriculture, Chinese Academy of Sciences, Changsha 410125, China

[2] Huanjiang Observation and Research Station for Karst Ecosystem, Chinese Academy of Sciences, Huanjiang, 547100, China

[3] University of Chinese Academy of Sciences, Beijng 100049, China

[4] Department of Geosciences and Natural Resource Management, University of Copenhagen, Copenhagen 1350, Denmark

*Corresponding authors:

Yuemin Yue (Email: ymyue@isa.ac.cn; Tel.: 86-0731- 84619701; Fax: 86-731-84612685)

and Kelin Wang (Email: kelin@isa.ac.cn; Tel.: 86-0731-84615201; Fax: 86-731-84612685)

Key Laboratory of Agro-ecological Processes in Subtropical Region, Institute of Subtropical Agriculture, Chinese Academy of Sciences, Changsha 410125, China

Abstract

Afforestation and land use changes have turned Southern China into one of the largest carbon sinks globally, which sequesters carbon from the atmosphere thus mitigating climate change. However, forest growth saturation and available land that can be forested limit the longevity of this carbon sink, and while a plethora of studies have quantified vegetation changes over the last decades, the remaining carbon sink potential of this area is currently unknown. Here, we train a model with multiple predictors characterizing the heterogeneous landscapes of Southern China and predict the carbon carrying capacity of the region for 2002-2017. We compare observed and predicted carbon density and find that during two decades of afforestation, 2.34 Pg C have been sequestered between 2002 and 2017, and a total of 5.32 Pg carbon can potentially still be sequestrated. This means that the region has reached 75% of its carbon carrying capacity in 2017, which is 12% more than in 2002, equal to a decrease of 0.83% per year. We identify potential afforestation areas that can still sequester 2.39 Pg C, while old and new forests have reached 87% of their potential with 1.85 Pg C remaining. Our work locates areas where vegetation has not yet reached its full potential but also shows that afforestation is not a long-term solution for climate change mitigation.

Key words: southern China; carbon carrying capacity; carbon sink potential; karst ecosystem.

1. Introduction

Global warming, resulting from human-induced emissions of greenhouse gases, not only increases the frequency of extreme climate events and causes the sea level to rise (IPCC, 2001; Benítez et al., 2007), but also leads to adverse environmental impacts, such as the reduction of vegetation productivity and biodiversity (Wu et al., 2020), significant losses of soil inorganic carbon (Song et al., 2021), and the disturbance of the natural carbon cycle (Reichstein et al., 2013). Forests sequester carbon dioxide from the atmosphere in the form of vegetation biomass, and are thus an effective way to reduce atmospheric carbon (Nunes et al., 2020; Zhang et al., 2021). The total global forest carbon stock is estimated to be 662 Pg C, of which ~45% are stored in living aboveground biomass (FAO, 2020), accounting for 70-80% of the total terrestrial carbon (Baccini et al., 2012). With increasing greenhouse gas emissions, reports such as the United Nations Framework Convention on Climate Change (UNFCCC) propose to invest in afforestation to remove carbon dioxide from the atmosphere. The regrowth of natural forests is considered as one of the most important natural climate solutions (Cook-Patton et al., 2020).

China has invested considerable effort in increasing vegetation coverage by forestation projects (Fang et al., 2018). By 2020, China has afforested a total of 6.77 million hectares (FAO, 2020; SFGA, 2020) leading to a total forest area of 220 million hectares, which accounts for 5% of the global forests (FAO, 2020). About 45% of these forests are concentrated in and around the karst region of southern China (Tong et al., 2020), making this area a global hot spot of vegetation growth (Tong et al., 2018; Brandt et al., 2018). Indeed, Tong et al (2020) have shown that land and forest management have removed an amount of carbon equivalent to 33% of the regional fossil fuel emissions over the last decade. Following massive plantation efforts, the forest growth of this area was remarkable (Tong et al., 2020), yet many studies indicate that carbon storage increases quickly in young forests, but reaches a relatively stable level in older forests (Wang et al., 2011; He et al., 2017; Yu et al., 2017; Zhang et al., 2017). Moreover, forest growth and carbon storage potential of the region are heterogeneous, depending on land use, forest stand age and type, as well as landscape and climate (Liu et al., 2014; He et al., 2017; Brandt et al., 2018; Liu et al., 2020; Tong et al., 2020; Cai et al., 2021). Consequently, while CO_2 emissions continue to increase, estimating the remaining carbon removal potential of Southern China's forests is important for ecological restoration strategies.

Estimating the potential of a forest to sequester carbon requires comparing its current state with its carbon carrying capacity, which is the amount of carbon that can be stored under prevailing environmental conditions (Roxburgh et al., 2006). Forest surveys and field observations are widely used to estimate the

carbon sequestration capacity under different growing and management scenarios (Lal and Singh, 1998; Roxburgh et al., 2006; Kumar. 2006; Udawatta and Jose, 2011; Macreadie et al., 2017; Tang et al., 2018; Cai et al., 2021). Liu et al., (2014) estimated the carbon carrying capacity in China based on 338 forest inventory sites in 2006, 2007, and 2010, and calculated a carrying capacity of 19.87 Pg C with a remaining potential of 13.86 Pg C. Cai et al., (2021) used the forest carbon sequestration model from 3365 forest survey plots, to assess the carbon sequestration rate of Chinese existing and new forests during 2010-2060. They found a carbon sequestration rate of 0.21 Pg C yr^{-1} over the period, with 11% of this sink coming from forestation. However, the application of these assessments based on field records in areas characterized by spatially heterogeneous landscapes and with a high forest dynamic, like Southern China, is challenging.

Multi-source satellite data and machine learning allow for a rapid assessment of carbon sequestration potentials at global and regional scales (Hamilton et al., 2018; Pascual et al., 2021; Ross et al., 2021). The prediction of the carbon sink potential is particularly important in forest plantation areas, such as in some parts of the Brazilian Amazon (Heinrich et al., 2021), the Hawaiian forest reserves (Pascual et al., 2021), or the Three-North Shelterbelt in China (Zhang et al., 2021). This is also the case for Southern China, where a heterogeneous landscape impedes generalized assumptions and requires locally calibrated models. A high level of details, including different land covers/uses, human disturbances as well as long-term observations covering larger areas are important to provide a scientific reference for regional policymakers and stakeholders evaluating and planning ecological protection measures.

Here we used 17 factors well describing the local landscape characteristics to predict the carbon carrying capacity of Southern China modeled at a 500 x 500 m resolution. We derived the per-pixel carbon sink potential by comparing the carbon carrying capacity with the observed carbon density (dataset available from Tong et al., (2020)) per grid cell for the years 2002-2017. We used annual forest maps to monitor changes in the carbon sink potential of old forests (always forest over 2002-2017), new forests (no forest in 2002 but in 2017) and potential forests (never forest over 2002-2017), and study the remaining carbon sink potential in 2017. The major objectives of this study were to assess to which extend forest growth has reached the limits of the carbon sink potential of Southern China over 2002-2017, to quantify the remaining carbon sink potential for different forest types in 2017, and to determine which factors influence the spatial patterns.

2. Materials and methodology

2.1 Study area

The study area (Fig. 1) is located in southern China and covers over 1.96 million km^2, including the provinces Hubei, Hunan, Guangdong, Guangxi, Guizhou, Yunnan, Sichuan, and Chongqing. The sloping landscape is characterized by a

variety of different karst formations, large variations in mean annual temperature (-14 to 25 °C) and rainfall (518-2235 mm), and decades of deforestation followed by decades of afforestation. Urbanization, rural depopulation, and ecological protection programs have reduced the agricultural use of the area, with about 29% still being croplands in 2020. A total of 28% of the region are covered by karst, which are often degraded landscapes subject to various ecological projects (Wang et al., 2019). A total of 71% of the croplands and urban areas are found in the non-karst area, which accounts for 70% of the region. Other major vegetation types are subtropical evergreen and deciduous broad-leaved forests (~50%) and grassland (~14%) (Wang et al., 2019). The Southeast margin of the Tibetan Plateau has an annually accumulated temperature lower than 2000°C and is not suited for forests, so we masked this study (CMA, 1978). We also masked croplands and urban areas (32% of the study area) as a reduction of croplands on the expense of additional afforestation would lead to unpredictable shortages in the food production. Croplands, urban and water areas were masked using the maps from Globeland30 from 2020 (30 x 30 m) (http://www.globeland30.org/).

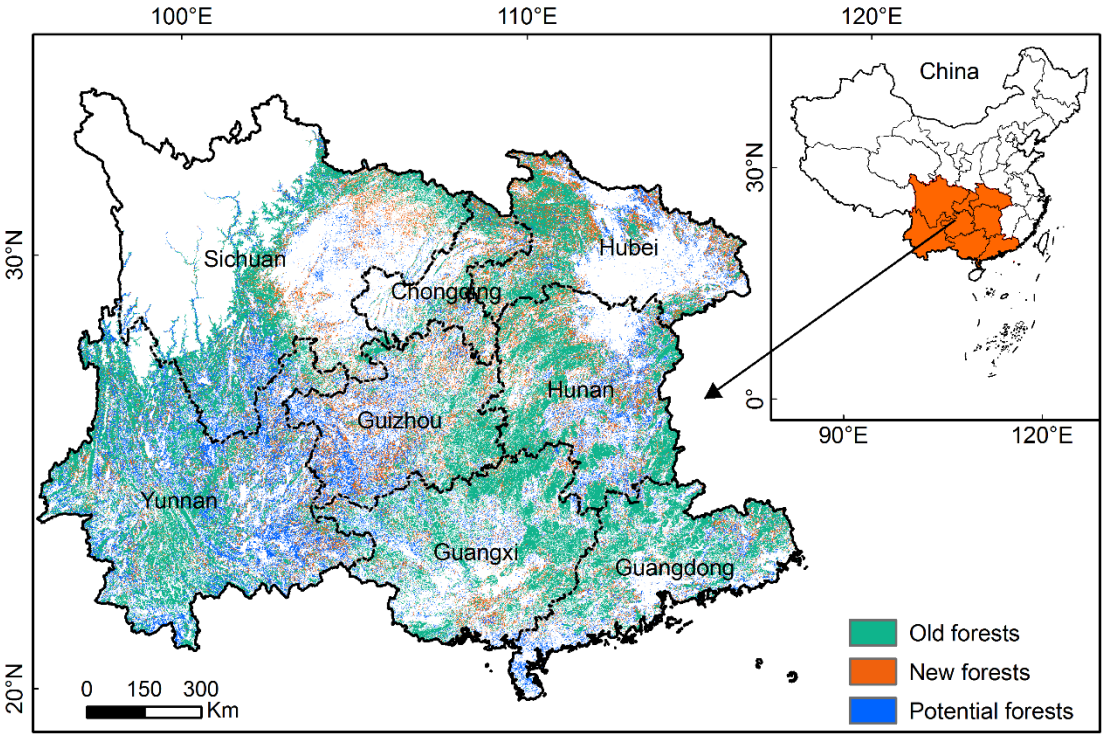

Fig.1 Study area and forest types. Annual forest data are from Tong et al., (2020). Old forests were forests during 2002-2017, new forests were forests in 2017 but not in 2002, and potential forests have not been forested during 2002-2017. Croplands, urban areas and the Southeast margin of the Tibetan Plateau

have been masked.

2.2 Annual C density and forest maps

Both the annual carbon density and annual forest maps are available at a resolution of 500 x 500 m for 2002-2017 from Tong et al., (2020). The annual carbon density of the study area uses boosted regression trees, which were trained with a static global benchmark map of carbon density of woody vegetation for 2018, using MODIS (MCD43A4 7 bands; NDII, EV12, MCD43A3 shortwave albedo) and STRM data. We refer to Tong et al., (2020) for details on the maps.

Annual forest maps were also derived from MODIS data. We identified three types of forests (Fig.1): (1) old forests (always forest during 2002-2017), (2) new forests (no forest in 2002 but in 2017), and potential forests (never forest during 2002-2017). Note that potential forests may include areas where forest growth is limited by natural factors.

2.3 Environmental data and the human influence intensity index

We used 17 environmental factors to predict the potential carbon density: Mean annual temperature (MAT), mean annual precipitation (MAP), 0°C annually accumulated temperature, 10°C annually accumulated temperature, and the aridity and humidity index. These data are available from the Research Center for Eco-Environmental Sciences, Chinese Academy of Sciences at 500 m resolution. Further data applied are maps on the lithology, geology, and the hydrological richness (obtained by summing the hydrological elements from the 1:1M scale national fundamental geographic map including rivers, lakes and springs), as well as geomorphological units, topography (DEM, slope, aspect) and soil properties (soil types, clay content, sand content and silt content).

The human influence intensity (HII) index proposed by Sanderson et al., (2002) was used. We applied a road distance map (https://www.openstreetmap.org/), a grided population density map from 2015 (1 km × 1 km) (https://www.resdc.cn/), nighttime lights from 2018 (500 m × 500 m) (https://dataverse.harvard.edu/) and land use data from 2020 (30 m × 30 m) (http://www.globeland30.org/) to generate the HII at 500 m × 500 m. We assigned scores to population density, roads and railways, land use/ cover, which were summed to quantify the HII, which ranges from 0.05 to 30 (Fig. S4).

2.4 Predicting the carbon carrying capacity

We selected all pixels with a carbon density value above the 75% quantile of each province resulting in a total number of 728,786 pixels. The stratification in provinces guarantees that diverse landscapes are covered (Table S1). Selecting only high values assumes that vegetation in these areas has reached a mature state representing values close to the carbon carrying capacity. Out of these values, we randomly selected 50,000 samples that were used to train a Random Forest model. The 17 environmental factors (previous section) were used as independent variables to predict the carbon carrying capacity for each 500 x 500 m pixel. The per-pixel prediction reflects the carbon carrying capacity of

individual factor combinations. To guarantee a robust model, we repeated the procedure 5 times with different random samples, thereby training 5 separate models. We used the average of the 5 models for the presentation of the results, and the difference between the models reflects the uncertainty. The average R^2 of the models was 0.92 and the average PMSE was 22.75 Mg C ha^{-1} and, MAE 15.12 Mg C ha^{-1}.

The difference between observed carbon density and the carbon carrying capacity is the potential carbon density. The observed carbon stocks / carbon carrying capacity in % shows how much of the carrying capacity has been reached during 2002-2017. Low percentage values imply that the area has not reached its carbon carrying capacity (corresponding to 100%).

2.5 The optimal parameter-based geographical detector (OPGD) model

Identifying the potential constraints of forest growth in different geographical settings is crucial to optimize actions to achieve the local carbon carrying capacity. The OPGD model was used to explore the dominant factors influencing the spatial patterns of carbon density for different forest types. The model consists of five parts: the factor detector, parameter optimization, the interaction detector, the risk detector, and the ecological detector (Song et al., 2020). The relative importance of factors determining the patterns of carbon density is quantified with a Q-value derived from the factor detector. The Q value of each factor is calculated as follows:

$$Q_v = \frac{\sum_{i=1}^{L} N_{v,i}\sigma_{v,i}^2}{N_v\sigma_v^2}$$

Where $N_{v,i}$ and $\sigma_{v,i}^2$ represent the number and the variance of C density in each of stratum, N_v and σ_v^2 represent the number and the variance of C density over the entire study area. The F-test is used to determine significant ($p<0.05$) differences among the stratified factors. The risk detector is used to search for areas with high observed and potential carbon density in the stratified factors. The differences between mean values of subregions can be compared using a t-test (Wang et al., 2017). The parameters optimization is used to determine the most suitable discretization method and break numbers, and it was also used for rainfall and temperature. For the HII, we used 5 levels: slight pressure (0.05<HII 9.67), light pressure (9.67<HII 11.20), moderate pressure (11.20<HII 14.84), severe pressure (14.84<HII 18.95), and extreme pressure (18.95<HII 30), based on the parameters optimization of the OPGD model (S4).

3. Results

3.1 Changes of potential carbon stocks

We calculated the difference between the predicted carbon carrying capacity, and the observed carbon stocks to reflect the potential carbon stocks, which is the amount of carbon that can potentially still be sequestered. The potential carbon stocks were calculated for the period 2002-2017 (Fig. 2a). Note that we did not include croplands and urban areas in these calculations. Our results show that forestation and associated carbon density gains decreased the remaining potential carbon density from 65.52 ± 2.41 Mg C ha^{-1} in 2002 to 45.41 ± 2.40 Mg C ha^{-1} in 2017, which is a decrease of -30.69% (Fig. 2b). More specifically, only 10.19% of the area has reached a saturated stage during the period, while 49.21% remain below their potential. This implies that 12.88 Pg C carbon had been sequestered before 2002, 2.34 Pg C during 2002-2017, and 5.32 Pg C carbon can still be sequestrated. In other words, 63.01% of the carbon carrying capacity was reached in 2002, while it is 75.39% in 2017 (Fig. 2c). Most carbon gains were observed in the mountains around the Chengdu Plain, as well as the karst regions of western Hubei, Hunan, Guizhou, and Guangxi (Fig. 2a). The center of the Yunnan-Guizhou Plateau (eastern Yunnan, Guizhou, and northwestern Guangxi) has the largest remaining carbon sink potential, highlighting this region as a target area for future ecological restoration projects, but also eastern Hunan and Hubei show a considerable remaining potential (Fig. 2a). The potential carbon stocks continuously declined from 2002 to 2017 with 0.15 ± 0.03 Pg C $year^{-1}$, following a polynomial fit (Fig. 2c). If the forest growth continues following this fit, the carbon carrying capacity would possibly be reached in 2029.

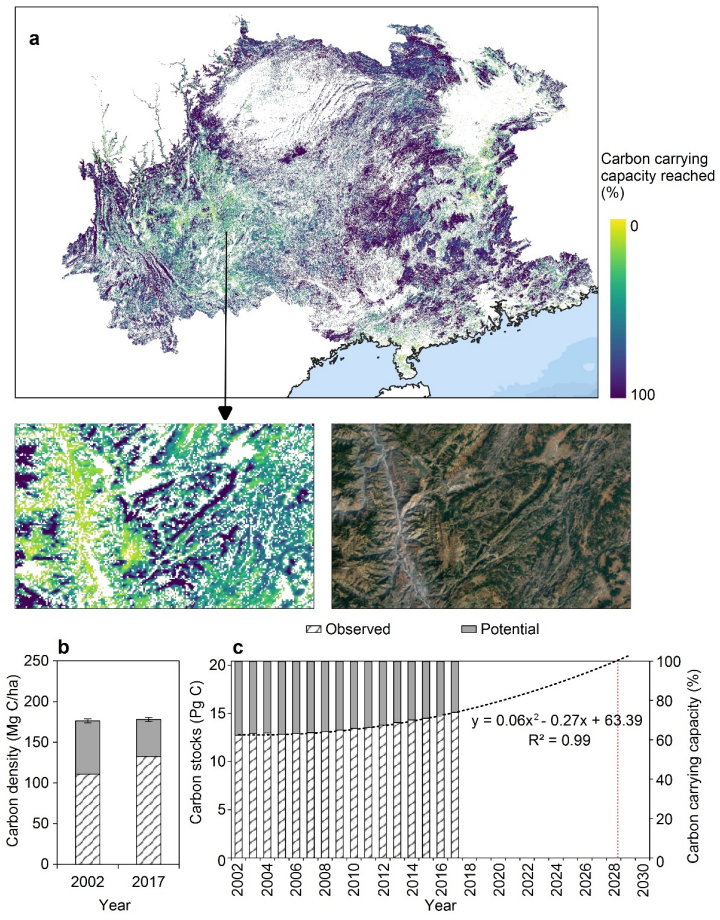

Fig. 2 Carbon sink potential in the research area. **a,** The % of the carbon

carrying capacity that was reached in 2017. Croplands and urban areas are masked. The satellite image is from GoogleEarth. **b,** Mean values of observed and potential carbon density in 2002 and 2017. The error bars reflect the differences between 5 model runs. **c,** Observed and potential carbon stocks at annual scale. The right y-axis shows how much of the carrying capacity has been reached during 2002-2017. A polynomial regression was fitted over the annual data.

3.2 Carbon sequestration potential for different forest types

We used annual forest maps generated by Tong et al (2020) to classify the study area into old forests (always forest during 2002-2017), new forests (no forest in 2002, but in 2017) and potential forests (never forest during 2002-2017). Potential forests, new forests, and old forests account for 10.91%, 8.23%, and 23.51% of the study area (Fig. 1, Fig. 3a). All three types show an overall decrease in potential carbon stocks over 2002-2017, implying that the observed carbon stocks are increasing (Fig. 3b-d). The strongest decrease of potential carbon density was found in new forests (2.59 Mg C ha^{-1} yr^{-1}, 25.19%), followed by potential forests (1.13 Mg C ha^{-1} yr^{-1}, 10.38%) and old forests (0.90 Mg C ha^{-1} yr^{-1}, 7.81%) (Fig. 3b, 3d). In 2017, potential forests have reached 42.41% of their carbon carrying capacity, with 2.39 Pg C (100.15 ± 2.87 Mg C ha^{-1}) potential carbon stocks remaining. New forests have reached 71.29% with 0.99 Pg C (19.21 ± 2.44 Mg C ha^{-1}) remaining, and old forests have reached 92.30% with 0.86 Pg C (47.84 ± 2.90 Mg C ha^{-1}) remaining. The potential carbon stocks decreased at the same rate in new forests (0.05±0.004 Pg C yr^{-1}) and old forests (0.05±0.01 Pg C yr^{-1}), followed by potential forests (0.03±0.004 Pg C yr^{-1}) (Fig. 3d). Overall, 9.75x10^4 km^2 (4.99 %) of the area has reached their carbon carrying capacity during the period: 12.31% (1.20 x 10^4 km^2) of the new forests and 84.92% (8.28 x 10^4 km^2) of the old forests (Fig. 3c). Non-karst areas showed a stronger decrease of potential carbon density in new forests (2.74 Mg C ha^{-1} yr^{-1}) as compared to karst areas (2.34 Mg C ha^{-1} yr^{-1}), but the values in old forests in karst area (1.04 Mg C ha^{-1} yr^{-1}) decreased faster than in non-karst areas (0.85 Mg C ha^{-1} yr^{-1}) (Fig. S3).

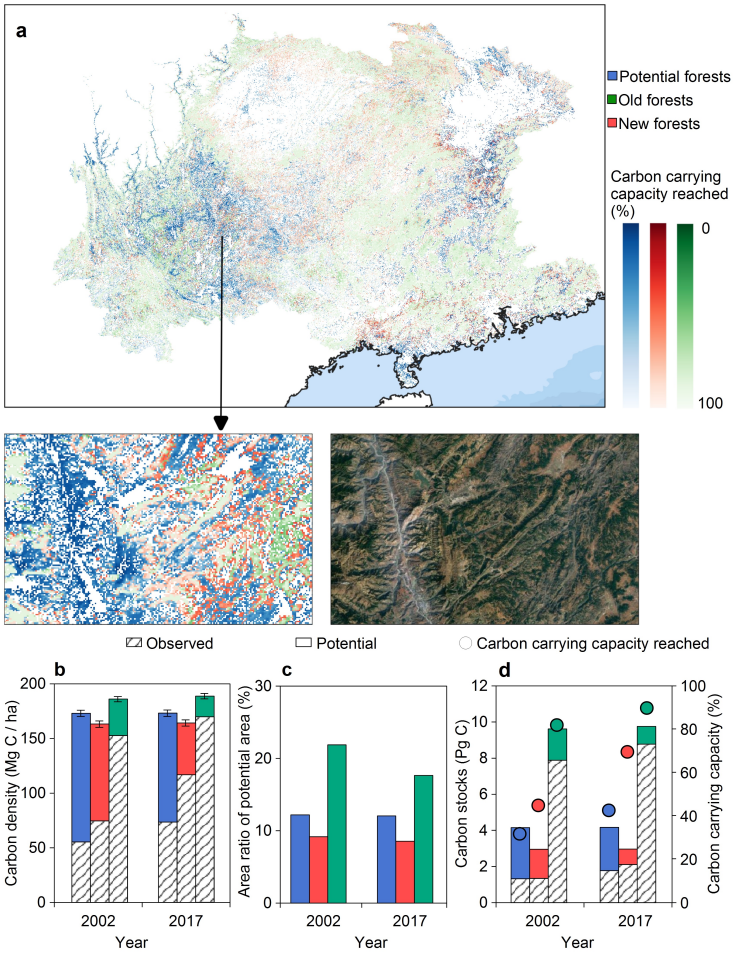
a
Potential forests
Old forests
New forests
Carbon carrying capacity reached (%)
0
100
Observed
Potential
Carbon carrying capacity reached
b
Carbon density (Mg C / ha)
200
150
100
50
0
2002
2017
Year
c
Area ratio of potential area (%)
30
20
10
0
2002
2017
Year
d
Carbon stocks (Pg C)
12
10
8
6
4
2
0
Carbon carrying capacity (%)
100
80
60
40
20
0
2002
2017
Year

Fig.3: Potential carbon sequestration in different forest types. **a,** The % of the carbon carrying capacity that was reached in different forest types in 2017. High values reflect a mature state of the vegetation. The satellite image is from GoogleEarth. **b,** Mean values of observed and potential carbon density in different forest types in 2002 and 2017. The error bars reflect the differences between 5 model runs. **c,** The proportion of areas with unsaturated carbon potential for different forest types in 2002 and 2017. **d,** Potential carbon stocks and the percent of carrying capacity for different forest types in 2002 and 2017.

3.3 Factors influencing potential and observed carbon density

We applied a factor detection (Q-value) to explore the drivers influencing potential and observed carbon density in southern China; note that croplands and urban areas are excluded (Fig. 4). The results show that the geographical setting is the major factor explaining the spatial patterns. With a Q value of 0.11, the terrain relief had the strongest influence on the spatial pattern of the potential carbon density, followed by soil types and slope, both with a Q value of 0.06. The observed carbon density was most influenced by elevation, with a Q value of 0.40. Climate conditions impact both potential and observed carbon density MAP mostly influenced the potential carbon density but not the observed carbon density, while it was the opposite for MAT. In addition, even though we excluded croplands and urban areas, the human influence factor had a clear influence on the spatial patterns of potential and observed carbon density, with Q values of 0.09 and 0.14, respectively. The influence of soil types on potential carbon density was almost the same as climate zones (0.06), but was stronger on observed carbon density (0.15).

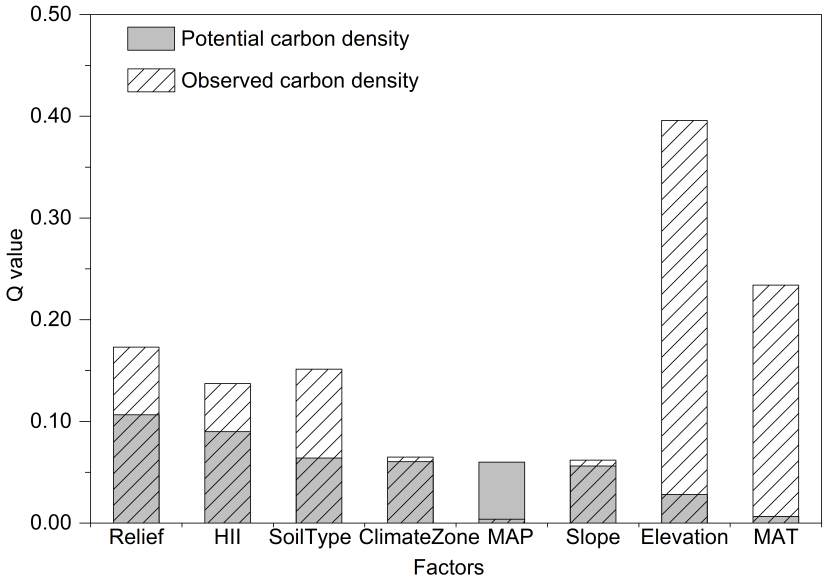

Fig.4 The relative importance of explanatory variables influencing the spatial

pattern of carbon density. Relief: Terrain relief; HII: Human influence intensity; MAP: Mean annual precipitation; Elevation: Digital Elevation Model; MAT: Mean annual temperature.

The spatial patterns of potential, observed, and predicted (=carrying capacity) carbon density vary with factors, and we compared averaged carbon density for different classes of each factor derived from the risk detector analysis (Fig. 5) (Song et al., 2020). The potential carbon density clearly decreases with increasing terrain relief (Fig. 5a) and increases with increasing human pressure (Fig. 5b), while it is the opposite for the observed carbon density. Observed carbon density in rough (Fig. 5a), remote (Fig. 5b), and sloping (Fig. 5f) areas was close to the carbon carrying capacity. The highest carbon carrying capacity and observed carbon density was found at an altitude between 2500 m and 3600 m (326.86 Mg C ha^{-1} and 263.72 Mg C ha^{-1}) (Fig. 5g), which coincides with the plateau climate zone (Fig. 5d) characterized by low mean annual temperature and alfisols (Fig. 5c). The highest average potential carbon density (117.60 Mg C ha^{-1}) was found in areas with semi-alfisols (Fig. 5c). Potential carbon density showed a greater spatial difference for various levels of MAP as compared to MAT, and the areas with the highest carbon potential were located for areas with MAP less than 1000 mm (Fig. 5e) while fewer differences were found for different MAT levels (Fig. 5h).

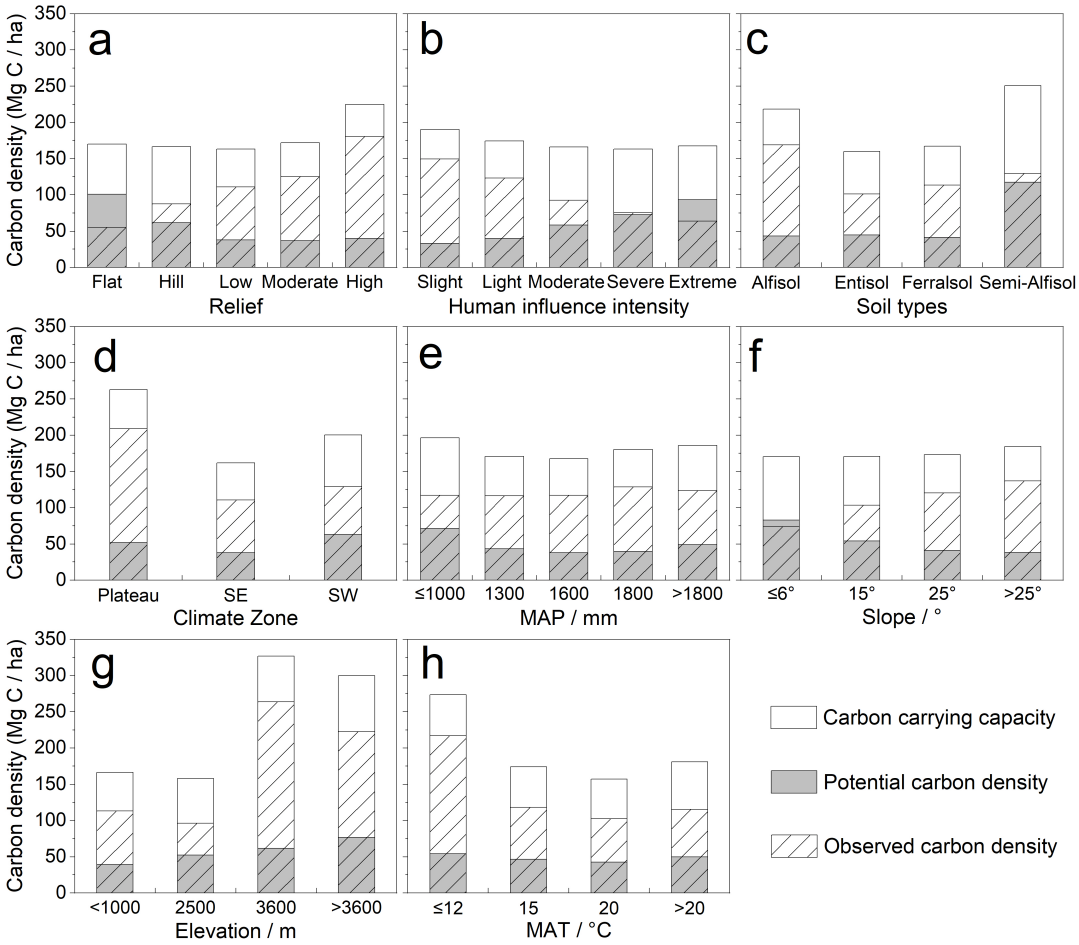

Fig.5 Average carbon density values for different classes of a, relief, b, human influence intensity, c, soil types, d, climate zones, e, mean annual precipitation (MAP), f, slope, g, elevation (DEM), and h, mean annual temperature (MAT). Observed + potential carbon density = carbon carrying capacity.

4. Discussion

4.1 A win-win situation by restoration projects

Promoting forest restoration and increasing tree cover is a nature-based climate solution and a possible way to mitigate global climate change by removing CO_2 from the atmosphere (Griscom et al., 2017; Doelman et al., 2020). Local projects restoring forests and planting trees are a crucial component of this pathway to sustainable carbon neutrality (Domke et al, 2020; Erbaugh et al., 2020; Wang et al., 2020). Over the past two decades, afforestation and ecological restoration

projects in Southern China have transformed large areas of croplands into forests (Yue et al., 2020), but about 5.3 Pg C can still be sequestered. According to Le Quéré et al, (2018), there are 42 Pg C potential carbon stocks globally in 2017, which would imply that about 12.6% of these are located in Southern China. However, the rapid growth of trees limits the remaining carbon stock potential of the region, making regular carbon stock inventories an important part of forestation projects.

Maximizing carbon uptake was not among the major aims when China's restoration projects were planned several decades ago. Rather poverty reduction, stopping the loss of top soil and rocky desertification as well as maximizing forest cover were key aims of the projects (Jiang et al., 2014; Hua et al. 2018b). The abandonment of croplands and the increase in forest cover can be regarded as environmental success, and our study shows that 75% of the carbon carrying capacity has been reached in 2017, which is 12% more than in 2002. The increase in carbon sequestration and other ecosystem services also benefits local livelihoods which is a win-win situation that not only addresses environmental problems and mitigates poverty, but also helps to combat climate change.

Our results uncover and quantify where vegetation has not yet reached its full potential, which is, not surprisingly, in non-forested areas, but also new forests which were planted in the frame of afforestation projects have only reached 71% of their potential in 2017, while old forests are close to their carbon carrying capacity (92%). A total of 58% of the remaining carbon stock potential is found in areas which are currently not forested mainly in the central of the Yunnan-Guizhou plateau, Nanling Mountains and the southeastern coastal areas of Guangdong. These areas should be the main target of future restoration programs, however, human interference, a harsh climate and fragile geological settings make a rapid recovery difficult (Wang et al., 2019; Yue et al., 2020). Potential forestation areas, include abandoned farmlands and mining areas, which are difficult to identify with coarse resolution imagery as used in this study, and require high-resolution images to precisely identify these areas.

Planted trees are usually selected based on the criteria of rapid growth and/or economic output, either by tree harvest or as cash crops. For example, fast growing *Eucalyptus* plantations rapidly generate revenues but do not provide the same ecological benefits as native forests (Hua et al., 2018a). Moreover, most forest plantations are not optimized to sustain long-term carbon stocks (Palmer, 2021), which explains why only 10% of the region has reached its carbon carrying capacity, in spite of intensive forestation. Future ecological projects could be adjusted towards fixing more CO_2 maximizing the full carbon sequestration potential of the region.

Consequently, to improve future ecological projects and rapidly reach the full carbon sequestration potential of an area, it is crucial to identify the potential constraints of forest growth as well as determine the land available for sustainable afforestation (Waring et al., 2020), natural regeneration and assistant reconstruction (Palmer, 2021).

4.2 How to make full use of the local carbon carrying capacity

We demonstrated that local terrain and human interference define the spatial patterns of vegetation carbon density in Southern China, which differs from other studies conducted at national and global scale, highlighting the importance of climatic factors (Jiao et al., 2021), such as temperature and precipitation. For southern China, the subtropical monsoon climate provides sufficient rainfall, so human activities, such as economic development, urban expansion, agriculture, but also ecological restoration projects determine the patterns of forests (Lu et al., 2018). The spatial distribution of human population density is influenced by terrain (Ma and He, 2021), with human activities mainly being concentrated in areas of low elevation, and flat terrain. We observed that observed and potential carbon density varied with the intensity of human interference and terrain, which can be interpreted by the following points. First, many croplands have been transformed into managed forests dominated by monocultures with a high remaining carbon sequestration potential. Second, native forests close to croplands and urban areas have often been replaced by afforestation areas yielding higher economic output, resulting in a decline of ecological benefits, such as biodiversity, carbon sequestration and water retention) (Ouyang et al., 2016; Hua et al., 2018a; 2018b). These areas usually have favorable natural conditions and efforts replacing monocultures with multiple species or assist natural regeneration could generate a potential carbon sink (Lamb et al. 2005). Also, bare areas resulting from construction and mining works have a certain carbon sink potential (Wang et al., 2018), but the restoration of these areas is challenging. Forests in protected areas with little human interference (NDRC, 2016) as well as forests in remote mountain areas are less disturbed and close to their carrying capacity with a lower carbon sequestration potential.

Soil types are important as well, and we found the highest carbon sink potential in semi-alfisols (Shi et al. 2010), which are mainly distributed in dry-hot valleys of the Hengduan Mountains, where plant growth is controlled by a special microclimate with high temperature and low rainfall (Yang et al., 2016). Native tropical valley monsoon forests have been degraded from human overuse and are difficult to recover in this dry area (Ma and McConchie 2001). Here, vegetation communities vary with elevation and slope (He et al., 2000), which requires adjusted ecological restoration measures (Zhang et al., 2003). Moreover, tropical and subtropical fruit could be introduced into this area (HKT, 2021), which would improve the region's economy and increase carbon sequestration.

In summary, the carbon sink potential in areas with a high human pressure and steep slope is still high. These areas have now been located and their potential has been quantified, it is now up to stakeholders to take action.

5. Conclusions

Forestation programs have been suggested as a measure to mitigate global climate change. Southern China has been subject to large-scale forestation activities over the past two decades, but the longevity of this carbon sink is rather

unknown. We find that 8% of the area has been forested during 2002-2017, consuming 12% of the carbon carrying capacity over the past two decades. This implies that the region has reached 75% of the carbon carrying capacity in 2017. However, previous forestation projects were designed to maximize forest cover but not carbon stocks, and future forestation programs need to make use of maps such as the one provided by this study to identify areas that are below their carbon carrying capacity. Moreover, planted tree species, tree density and harvest cycles can be adjusted to generate a long-term and sustainable carbon sink making use of the local carbon carrying capacity of a given area. However, we also show that afforestation provides only a short-term solution as climate change mitigation measure and only a reduction of CO_2 emissions can mitigate climate change in the long term.

Acknowledgements

This study was funded by the National Key Research and Development Program of China (2018YFD1100103), the National Natural Science Foundation of China (41930652, U20A2048), the Marie Curie fellowship (795970) and the China Scholarship Council (CSC202004910531). M.B. received funding from the DFF Sapere Aude (9064-00049B) and the European Research Council (ERC) under the European Union's Horizon 2020 Research and Innovation Programme (grant agreement no. 947757 TOFDRY). We thank http://www.naturalearthdata.com for providing background maps. All data sets are freely available: Both the annual carbon density and annual forest maps are available from Tong et al., (2020). The climate data (MAP, MAT, 0°C annually accumulated temperature, 10°C annually accumulated temperature, climate zones the aridity and humidity index), soil properties (soil types, clay content, sand content and silt content) and population density in 2015 will be available at the Research Center for Eco-Environmental Sciences, Chinese Academy of Sciences (https://www.resdc.cn/). The geological elements can be found at https://geocloud.cgs.gov.cn/. Roadmap in shapefile format can be downloaded at https://www.openstreetmap.org/, nighttime lights at https://dataverse.harvard.edu/, and land use data at http://www.globeland30.org/.

References

Baccini A., Goetz S. J., Walker W. S., Laporte N. T., Sun M., Sulla-Menashe D., et al. (2012). Estimated carbon dioxide emissions from tropical deforestation improved by carbon-density maps. Nature Climate Change 2:182-185. https://doi.org/10.1038/nclimate1354

Benítez P. C., McCallum I., Obersteiner M., & Yamagata Y. 2007. Global potential for carbon sequestration: Geographical distribution, country risk and policy implications. Ecological Economics 60:572-583. https://doi.org/10.1016/j.ecolecon.2005.12.015

Brandt M., Yue Y. M., Wigneron J. P., Tong X. W.,Tian F., Jepsen, M. R., et al. (2018). Satellite-Observed Major Greening and Biomass Increase in South

China Karst During Recent Decade. Earths Future 6:1017-1028.

Cai, W. X., He N. P., Li M. X., Xu L., Wang, L.Z., Zhu J. H., et al., 2021. Carbon sequestration of Chinese forests from 2010–2060: spatiotemporal dynamics and its regulatory strategies. Science Bulletin. https://doi.org/10.1016/j.scib.2021.12.012

China Meteorological Administration (CMA). (1978). Climate regionalization in China. https://www.resdc.cn/data.aspx?dataid=243

Cook-Patton S. C., Leavitt S. M., Gibbs D., et al. (2020). Mapping carbon accumulation potential from global natural forest regrowth. Nature 585:545-550. https://doi.org/10.1038/s41586-020-2686-x

Doelman J. C., Stehfest E., van Vuuren D. P., et al. (2020). Afforestation for climate change mitigation: Potentials, risks and trade-offs. Global Change Biology 26:1576-1591. https://doi.org/10.1111/gcb.14887

Domke G. M., Oswalt S. N., Walters B. F., & Morin R. S. (2020). Tree planting has the potential to increase carbon sequestration capacity of forests in the United States. Proceedings of the National Academy of Sciences 117:24649. http://doi.org/10.1073/pnas.2010840117

Erbaugh J. T., Pradhan N., Adams J., Oldekop J. A., Agrawal A., Brockington D., Pritchard R., & Chhatre A. (2020). Global forest restoration and the importance of prioritizing local communities. Nature Ecology & Evolution 4:1472-1476. https://doi.org/10.1038/s41559-020-01282-2

Fang, J., Yu G., Liu L., Hu S., & Chapin F. S. (2018). Climate change, human impacts, and carbon sequestration in China. PNAS 115:4015-4020. http://doi.org/10.1073/pnas.1700304115

FAO. (2020). Global Forest Resources Assessment 2020 – Key findings. Rome. https://doi.org/10.4060/ca8753en.

Griscom B. W., Adams J., Ellis P. W., et al. (2017). Natural climate solutions. Proceedings of the National Academy of Sciences 114:11645. https://doi.org/10.1073/pnas.1710465114

Hamilton, S. E., & Friess D. A. (2018). Global carbon stocks and potential emissions due to mangrove deforestation from 2000 to 2012. Nature Climate Change 8:240-244. https://doi.org/10.1038/s41558-018-0090-4

He, N. P., Wen D., Zhu J. X., Tang X. L., Xu L., Zhang L., Hu H., Huang M., & Yu G. (2017). Vegetation carbon sequestration in Chinese forests from 2010 to 2050. Global Change Biology 23:1575-1584. https://doi.org/10.1111/gcb.13479

He Y. B., Lu P. Z., & Zhu T. (2000). Causes for the formation of dry-hot valleys in Hengduan Mountain--Yunnan Plateau. Resources Science 22:69-72.

Heinrich, V. H., Dalagnol R., Cassol H. L., Rosan, T. M., de Almeida, C. T., Junior, C. S., et al. (2021). Large carbon sink potential of secondary forests

in the Brazilian Amazon to mitigate climate change. Nature Communications 12:1-11. https://doi.org/10.1038/s41467-021-22050-1

HKT. (2021). Dry and hot valley: a special microclimate that breaks the boundaries of plant growth. iNEWS, Nature. https://inf.news/en/nature/0c5487c3eaaf453d6156a5dc78f3e113.html

Hua F. Y., Wang L., Fisher B., Zheng, X. L., Wang, X. Y., Yu, D. W., et al. (2018a). Tree plantations displacing native forests: The nature and drivers of apparent forest recovery on former croplands in Southwestern China from 2000 to 2015. Biological Conservation 222:113-124. https://doi.org/10.1016/j.biocon.2018.03.034

Hua F. Y., Xu J. C., & Wilcove D. S. (2018b). A New Opportunity to Recover Native Forests in China. Conservation Letters 11: e12396. https://doi.org/10.1111/conl.12396

Jiang, Z. C., Lian Y. Q., & Qin X. Q. (2014). Rocky desertification in Southwest China: Impacts, causes, and restoration. Earth-Science Reviews 132:1-12. https://doi.org/10.1016/j.earscirev.2014.01.005

Jiao, W. Z., Wang L. X., Smith W. K., Chang Q., Wang H. L., & D'Odorico P. (2021). Observed increasing water constraint on vegetation growth over the last three decades. Nature Communications 12:3777. https://doi.org/10.1038/s41467-021-24016-9

Kumar, B. (2006). Carbon sequestration potential of tropical homegardens. Tropical Homegardens. Springer: 185-204. https://doi.org/10.1007/978-1-4020-4948-4_11

Lamb D., Erskine Peter D., & Parrotta John A. (2005). Restoration of Degraded Tropical Forest Landscapes. Science 310:1628-1632. https://doi.org/10.1126/science.1111773

Le Quéré, C., Andrew, R. M., Friedlingstein, P., Sitch, S., Hauck, J., Pongratz, J., et al. (2018). Global Carbon Budget 2018. Earth System Science Data 10: 2141–2194. https://doi.org/10.5194/essd-10-2141-2018

Liao, C. J., Yue Y. M., Wang K., Fensholt R., Tong X. W., & Brandt, M. (2018). Ecological restoration enhances ecosystem health in the karst regions of southwest China. Ecological Indicators 90:416-425. https://doi.org/10.1016/j.ecolind.2018.03.036

Liu, F. Y., Li K., Sun Y. Y., Tang G. Y, & Zhang C. H. (2010). Effects of climate on vegetation recovery in dry-hot valleys of Hengduan Mountains region in southern China. Resources and Environment in the Yangtze Basin 19:1386-1391.

Liu, Y. C., Yu G. R., Wang Q. F., Zhang Y. J., & Xu Z. H., et al. (2014). Carbon carry capacity and carbon sequestration potential in China based on an integrated analysis of mature forest biomass. Science China Life Sciences 57:1218-1229. https://doi.org/10.1007/s11427-014-4776-1

López-Pujol J., Zhang F. M., Sun H.Q., Ying, T. S., & Ge, S. (2011). Mountains of southern China as "plant museums" and "plant cradles": Evolutionary and conservation insights. Mountain Research and Development 31:261-269. https://doi.org/10.1659/MRD-JOURNAL-D-11-00058.1

Lu, F., Hu H. F., Sun W. J., Zhu J.J., Liu G. B., Zhou, W. M., et al. (2018). Effects of national ecological restoration projects on carbon sequestration in China from 2001 to 2010. PNAS 115:4039-4044. https://doi.org/10.1073/pnas.1700294115

Ma, C., & He, Y. (2021). Spatiotemporal Trends and Ecological Determinants in Population by Elevation in China Since 1990. Chinese Geographical Science 31:248-260. https://doi.org/10.1007/s11769-021-1188-6

Ma, H. C., & McConchie J. A. (2001). The dry-hot valleys and forestation in southwest China. Journal of Forestry Research 12:35-39. https://doi.org/10.1007/BF02856797

Macreadie, P. I., Ollivier Q. R., Kelleway J. J., Serrano O., Carnell P. E., Ewers Lewis C. J., & et al. (2017). Carbon sequestration by Australian tidal marshes. Sci Rep 7:44071. https://doi.org/10.1038/srep44071

National Development and Reform Commission (NDRC), People's Republic of China. (2016). The 13th Five-Year Construction Plan for the Comprehensive Control Project of Rocky Desertification in Karst Areas, 17-18.

Nunes, L. J. R., Meireles C. I. R., Pinto Gomes C. J., & Almeida Ribeiro N. M. C. (2020). Forest Contribution to Climate Change Mitigation: Management Oriented to Carbon Capture and Storage. Climate 8:21. https://doi.org/10.3390/cli8020021

Palmer, L. (2021). How trees and forests reduce risks from climate change. Nature Climate Change 11:374-377. https://doi.org/10.1038/s41558-021-01041-6

Pascual, A., Giardina C. P., Selmants P. C., Laramee L. J., & Asner G. P. (2021). A new remote sensing-based carbon sequestration potential index (CSPI): A tool to support land carbon management. Forest Ecology and Management 494:119343. https://doi.org/10.1016/j.foreco.2021.119343

Reichstein, M., Bahn M., Ciais P., Frank D., Mahecha M. D., Seneviratne S. I., et al. (2013). Climate extremes and the carbon cycle. Nature 500:287-295. https://doi.org/10.1038/nature12350

Roxburgh, S. H., Wood S. W., Mackey B. G., Woldendorp G., Gibbons P. (2006). Assessing the carbon sequestration potential of managed forests: a case study from temperate Australia. Journal of Applied Ecology 43:1149-1159. https://doi.org/10.1111/j.1365-2664.2006.01221.x

Sanderson, E.W., Jaiteh, M., Levy, M.A., Redford K. H., Wannebo A. V., Woolmer G. (2002). The human footprint and the last of the wild. Bioscience 52, 891– 904. https://doi.org/10.1641/0006-3568(2002)052[0891:THFATL]2.0.CO;2

State Forestry Administration (SFA). (2016). SFA's opinion on regulating the circulation market of collective forests, http://www.forestry.gov.cn/main/5925/20200414/090421590890271.htm

Shi X. Z., Yu D. S., Xu S. X., Warner E. D., Wang H. J., Sun W. X., Zhao Y. C., & Gong Z. T. (2010). Cross-reference for relating Genetic Soil Classification of China with WRB at different scales. Geoderma 155:344-350. https://doi.org/10.1016/j.geoderma.2009.12.017

State Forestry and Grassland Administration (SFGA). (2020). Communiqué on China's Land Greening Status in 2020.

Song X. D., Yang F., Wu H.Y., Zhang J., Li D. C., Liu F., et al. (2021). Significant loss of soil inorganic carbon at the continental scale. National Science Review. https://doi.org/10.1093/nsr/nwab120

Song Y. Z., Wang J. F., Ge Y., & Xu C. D. (2020). An optimal parameters-based geographical detector model enhances geographic characteristics of explanatory variables for spatial heterogeneity analysis: cases with different types of spatial data. GIScience & Remote Sensing 57:593-610. https://doi.org/10.1080/15481603.2020.1760434

State Forestry and Grassland Administration, Communiqué on the State of China's Land and Greening in 2020. http://www.forestry.gov.cn/main/393/20210312/175043478886085.html

Tang, X., Zhao X., Bai Y., Tang Z. Y., Wang W.T., Zhao Y.C., et al. (2018). Carbon pools in China's terrestrial ecosystems: New estimates based on an intensive field survey. PNAS 115:4021-4026. https://doi.org/10.1073/pnas.1700291115

Tong, X., Brandt M., Yue Y., Horion S., Wang K. L, Keersmaecker W. D., et al. (2018). Increased vegetation growth and carbon stock in China karst via ecological engineering. Nature Sustainability 1.

Tong, X., Brandt M., Yue Y., Ciais P., Rudbeck J. M., Penuelas J., et al. (2020). Forest management in southern China generates short term extensive carbon sequestration. Nature Communications 11:129. https://doi.org/10.1038/s41467-019-13798-8

Udawatta R.P. & Jose S. (2011). Carbon Sequestration Potential of Agroforestry Systems. Advances in Agroforestry 8 8. https://doi.org/10.1007/978-94-007-1630-8_2

Wang H., Zhang B., Bai X., & Shi L. (2018). A novel environmental restoration method for an abandoned limestone quarry with a deep open pit and steep palisades: a case study. Royal Society Open Science 5:180365. https://doi.org/10.1098/rsos.180365

Wang, J., Feng L., Palmer P. I., Liu Y., Fang S. X., Bösch H., et al. (2020). Large Chinese land carbon sink estimated from atmospheric carbon dioxide data. Nature 586:720-723. https://doi.org/10.1038/s41586-020-2849-9

Wang, J. F., & Xu C D. (2017). Geodetector: Principle and prospective. Acta Geographica Sinica 72:116-134. https://doi.org/10.11821/dlxb201701010

Wang, K. L., Zhang C. H., Chen H. S., Yue Y. M., Zhang W., Zhang M. Y., et al. (2019). Karst landscapes of China: patterns, ecosystem processes and services. Landscape Ecology 34:2743-2763. https://doi.org/10.1007/s10980-019-00912-w

Wang, S., Zhou L., Chen J., Ju W. M., Feng X. F., Wu W. X., (2011). Relationships between net primary productivity and stand age for several forest types and their influence on China's carbon balance. Journal of Environment Management 92:1651-1662. https://doi.org/10.1016/j.jenvman.2011.01.024

Waring B., Neumann M., Prentice I. C., Adams M., Smith P., & Siegert M. (2020). What role can forests play in tackling climate change? Imperial College London.

Wu, G.L., Cheng Z., Alatalo J. M., Zhao J. X., Liu Y. (2021). Climate Warming Consistently Reduces Grassland Ecosystem Productivity. Earth's Future 9:e2020EF001837. https://doi.org/10.1029/2020EF001837

Yang J. D., Zhang Z.M., Shen Z. H., Ou X. K., Geng Y. P., & Yang M. Y. (2016). Review of research on the vegetation and environment of dry-hot valleys in Yunnan. Biodiversity Science 24:462–474. https://doi.org/10.17520/biods.2015251

Yu, Y., Chen J. M., Yang X., Fan W., Fan W. Y., Li, M. Z.,He L. M. (2017). Influence of site index on the relationship between forest net primary productivity and stand age. PLOS One 12:e0177084. https://doi.org/10.1371/journal.pone.0177084

Yue Y. M., Liao C. J., Tong X. W., Wu Z. B., Fensholt R., Prishchepov A., Jepsen M. R., Wang K. L., & Brandt M. (2020). Large scale reforestation of farmlands on sloping hills in South China karst. Landscape Ecology 35:1445-1458. https://doi.org/10.1007/s10980-020-01026-4

Zhang, D. N., Zuo X. X., & Zang C. F. (2021a). Assessment of future potential carbon sequestration and water consumption in the construction area of the Three-North Shelterbelt Programme in China. Agricultural and Forest Meteorology 303:108377. https://doi.org/10.1016/j.agrformet.2021.108377

Zhang Y., Yao Y., Wang X., Liu Y., & Piao S. (2017). Mapping spatial distribution of forest age in China. Earth and Space Science 4:108-116. https://doi.org/10.1002/2016EA000177

Zhang, X. B., Yang, Z. & Zhang J. P. (2003). Lithologic types on hill slopes and revegetation zoning in the Yuanmou hot and dry valley. Scientia Silvae Sinicae 39:16-22. https://doi.org/10.11707/j.1001-7488.20030403